Available online at www.sciencedirect.com
ScienceDirect
Journal of Power Sources 175 (2008) 495–501
JOURNAL OF POWER SOURCES
www.elsevier.com/locate/jpowsour

Factors affecting the electrochemical reactivity vs. lithium of carbon-free $LiFePO_4$ thin films

F. Sauvage, L. Laffont, J.-M. Tarascon, E. Baudrin *

Laboratoire de Réactivité et Chimie des Solides, UMR CNRS 6007, Université de Picardie Jules Verne, 33 rue St. Leu, 80039 Amiens Cedex, France

Received 6 August 2007; received in revised form 7 September 2007; accepted 23 September 2007
Available online 2 October 2007

Abstract

The electrochemical stability of various current collector materials such as Si, Pt, 304 stainless steel, Ti, Al exposed to the most common lithium-ion electrolyte salts ($LiPF_6$, $LiBF_4$, $LiAsF_6$, LiTFSI, $LiClO_4$) have been herein investigated. For applied potentials greater than 3 V, the acidic fluorine-based electrolytes were shown to be the most corrosive. Consequently, aqueous and non-aqueous electrolytes (1 M $LiNO_3/H_2O$ vs. 1 M $LiClO_4$/EC-DMC) were successfully applied to study the electrochemical properties of C-free $LiFePO_4$ thin films whose redox potential is near 3.5 V vs. Li^+/Li^0. Using aqueous electrolyte has resulted in a lowering of both cell resistance and interfacial charge transfer resistance by almost one order of magnitude, hence enabling to considerably increase the electrochemical capacity of our $LiFePO_4$ thin films. Besides, we unravel the importance of the mechanical strains at the substrate/$LiFePO_4$ thin film interface on the film textural, structural modification and electrochemical stability upon cycling.

Keywords: Thin films; Pulsed laser deposition; $LiFePO_4$; Electrolyte; Cycling

1. Introduction

Since the commercialisation of the $LiCoO_2$/graphite system by Sony in 1991, "lithium-ion batteries" have remarkably invaded the market of the portable electronic devices and are expected to be the best candidate for Hybrid Electric Vehicle (HEV)/Electric Vehicle applications. However, present Li-ion technology falls short in meeting energy storage demands required by the automotive industry both in terms of performances and cost. That is why alternative redox materials displaying higher performances (e.g. high capacity and stability) with low cost and low toxicity are required. The 1997 Padhi et al.'s [1] report on the electrochemical activity of $LiFePO_4$-based cathodes constitutes one of the first steps towards the search for more environmentally friendly systems. Following such a finding, Ravet et al. [2] demonstrated that electrodes made of such low conducting $LiFePO_4$ materials could be an alternative to $LiCoO_2$ electrodes. This was realised by improving the material conductivity through the preparation of C/$LiFePO_4$ composites using carbon nanopainting techniques. Combining coatings with processes aimed towards lowering the particle size [3,4], nanosize coated $LiFePO_4$-based electrodes were successfully prepared and implemented, as alternative to $LiCoO_2$-based electrodes found in today's Li-ion cells for the HEV and power tools markets. Aiming to better understand the fundamental aspects governing the electrochemical properties of such olivine type material, we have recently undertaken the study of this system through a thin film approach [5], showing particularly that the morphology of the films [6] together with the choice of the preparation route (one step vs. two step deposition process) [7] influence largely its electrochemical reactivity. However, the obtained capacities were far from the theoretical ones, reaching solely 40% for well-structured films. This raised the question about the origin of such limited capacities, besides the low electronic and ionic conductivities arguments previously considered. To grasp further insight on such an issue, we have looked at the factors affecting the material electrochemical activity. We particularly compared the electrochemical kinetic of lithium insertion/de-insertion of $LiFePO_4$ both in organic and aqueous electrolyte using the C-free films grown by pulsed laser

* Corresponding author. Tel.: +33 322827971; fax: +33 322827590.
E-mail address: emmanuel.baudrin@u-picardie.fr (E. Baudrin).

0378-7753/$ – see front matter © 2007 Elsevier B.V. All rights reserved.
doi:10.1016/j.jpowsour.2007.09.085

deposition (PLD). Furthermore, our group [5] and other reports [8,9] have shown that $LiFePO_4$ is rechargeable in aqueous media. In such electrolytes, enhanced kinetic of the electrochemical phenomena has been previously reported for the spinel $Li_{1-x}Mn_2O_4$ most likely because of a larger electrolyte ionic conductivity together with the absence of a solid electrolyte interphase (SEI) [10]. In the present study, we further address different fundamental points essential when studying electrode materials thin films together with the aforementioned kinetic limitations. This paper is more specifically geared towards (i) identifying the most adequate non-aqueous electrolytes so as to ensure minimum corrosion of the films substrate during electrochemical testing, (ii) comparing the electrochemical kinetics in aqueous electrolyte compared to non-aqueous, (iii) measuring the electrochemical performance of dense carbon-free $LiFePO_4$ thin films together with the evolution of their microstructure upon cycling.

2. Experimental

Electrolytes based on 1 M $LiPF_6$, $LiAsF_6$, $LiClO_4$ or $LiBF_4$ in a mixture of ethylene carbonate/dimethyl carbonate (EC/DMC: 1/1) were obtained from Merck (selectipur@ grade). The lithium bis(trifluoromethanesulfonyl)imide (LiTFSI)-based electrolyte was prepared by dissolving this salt in a Merck selectipur@ mixture of EC and DMC 1:1 (v/v). For the study of the electrolyte reactivity with Si, a 10 nm thick Pt current collector was sputtered under vacuum at ambient temperature upon *n*-Si(0 0 1) substrate (Sb doped). Al, Ti, 304 stainless steel substrates were cut at the desirable dimensions (about 1.5 cm × 1 cm), mechanically polished up to a mirror-like quality and successively ultrasonically washed in ethanol and acetone. The growth of carbon-free crystallized $LiFePO_4$ thin films was performed by PLD [5]. A 80% dense $LiFePO_4$ target was prepared by annealing a pellet pressed at 2000 bar under isostatic conditions [6] at 800 °C under Ar for 24 h. The deposition process was conducted with a pulsed KrF excimer laser beam (Lambda Physik Compex 102, $\lambda = 248$ nm) at a 10 Hz frequency under 8×10^{-2} mbar of argon. The laser fluency and the target/substrate distance were 2 J cm^{-2} and 3 cm, respectively.

The films morphology was investigated using scanning electron microscopy (Philips XL30FEG). High resolution transmission electron microscopy (HRTEM—FEI TECNAI F20 S-TWIN) was used to evaluate the structural and textural evolution of the film upon cycling. The samples were obtained by peeling of the thin films and depositing the resulting powder on copper grids coated with lacey-carbon film. The film thicknesses were evaluated by profilometry using a Dektak ST3 model.

All the electrochemical measurements were recorded using a three-electrode configuration and monitored by an automatic multi-potentiostat system (VMP—Biologic SA, Claix, France) in a dry Ar backfilled glove box containing less than 1 ppm of water. A saturated Calomel electrode (SCE) and a Pt strip were used both as reference and counter electrodes in aqueous medium. In organic electrolyte, two lithium metal strips serve as counter and reference electrode. The distance between the electrodes was fixed at around 2 cm for all the experiments to allow a good comparison of the data between aqueous and non-aqueous electrolytes.

3. Results and discussion

3.1. Compatibility between lithium-based electrolytes and substrates

The effect of electrochemical side-reaction of substrate (current collector) with the electrolyte is crucial when studying thin film electrodes because of the low amount of active material present. The current linked to the parasitic reaction can easily be of the same order or higher than the studied phenomenon, rendering the study impossible. We first focused on a Si/Pt substrate, commonly used in thin film deposition for devices implementation. Fig. 1 shows the voltamperograms collected using different salt-based electrolyte in EC/DMC between 3 V and 4.5 V vs. Li^+/Li. While $LiPF_6$ EC/DMC is known to be stable up to 4.8 V [11], we observe the presence of a non-negligible anodic current around 3.8 V on *n*-Si/Pt which reaches a density of 1 mA cm^{-2} at 4.5 V. Furthermore, in the 3–4 V (vs. Li^+/Li) domain, a parasitic current of few tenth of μA cm^{-2} is also observed. Using a $LiBF_4$-based electrolyte, a similar behaviour was observed with an even lower onset critical potential (≈3.2 V) giving rise to a parasite current density of 0.5 mA cm^{-2} between 4.1 V and 4.5 V. On the other hand, $LiAsF_6$, $LiClO_4$ and LiTFSI-based electrolytes lead to almost negligible currents below 4.2 V, with therefore an exponential-like increase of the current beyond. These three latter salts thus appear suitable for the study of cathode materials, deposited on n-Si/Pt substrates, having redox potentials less than 4 V.

Over noble metals, it is known that above 3.5 V vs. Li^+/Li alkyl carbonate-based electrolytes can be oxidized [12]. However, this is not the only probable origin for the appearance of such anodic current since we noticed an evolution of the substrate surface morphology after only one electrochemical cycle (Fig. 2). It evolves from a smooth surface to a honeycomb-like

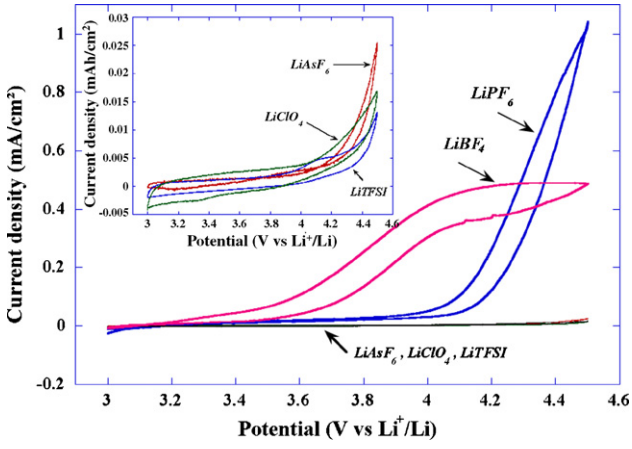

Fig. 1. Cyclic voltamperograms recorded at v = 2 mV s^{-1} scan rate between 3 V and 4.5 V (vs. Li^+/Li) of a *n*-Si (0 0 1)/Pt electrode in different electrolytes (1 M $LiPF_6$, $LiBF_4$, $LiAsF_6$, $LiClO_4$ and LiTFSI, EC/DMC). In inset, a zoom in the cyclic voltamperograms recorded using $LiClO_4$, $LiAsF_6$ and LiTFSI.

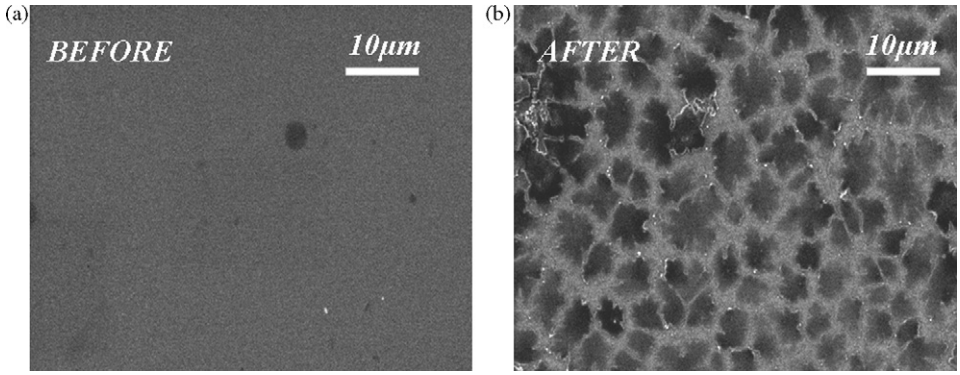

Fig. 2. SEM micrographs of the *n*-Si/Pt electrode before and after one cycle performed by cyclic voltamperometry in 1 M $LiPF_6$EC/DMC 1:1.

rough surface with holes size ranging from 5 μm to 10 μm of diameter suggesting a corrosion reaction-type process linked to the electrolyte salt nature and involving solvent decomposition. Such results did not come as a surprise knowing the well-known equilibriums (listed below) established for $LiPF_6$ and $LiBF_4$ solvated ions [13,14]:

$$Li_{(solv)}{}^{+} + PF_{6(solv)}{}^{-} \Leftrightarrow LiF_{(s)} + PF_{5(g)} \quad (1)$$

$$Li_{(solv)}{}^{+} + BF_{4(solv)}{}^{-} \Leftrightarrow LiF_{(s)} + BF_{3(g)} \quad (2)$$

We added some LiF salt (quasi-insoluble) into the electrolyte to try to displace the equilibrium but no drastic evolution was observed enabling us to rule out the influence of LiF or the lewis acid (PF_5 or BF_3) on the observed corrosion reaction. Another possibility lies in the presence of HF traces in these electrolytes keeping in mind that the solvated ion $PF_6{}^{-}$ strongly reacts with water traces (very difficult to suppress) yielding to the production of two HF molar equivalent according to [13]:

$$Li_{(solv)}{}^{+} + PF_{6(solv)}{}^{-} + H_2O \rightarrow 2HF + POF_3 + LiF \quad (3)$$

Such HF-driven corrosion is currently used for the electrochemical formation of macro and mesopores on doped silicon wafer in dilute $HF_{(aq)}$ with similar morphological observations [15,16]. Furthermore, the absence of HF traces in $LiAsF_6$-based electrolyte could be consistent with the inactivity of the latter on silicon substrate [14]. Similar cyclic voltamperometry experiments were performed for different metallic substrates: 304 stainless steel (304SS), Al and Ti. For conciseness reasons, we have summarized the electrolyte/substrates compatibility results in Table 1. As a result, we have obviously highlighted the advantage of using $LiClO_4$ as no electrochemical reactivity was experienced, regardless of the substrate nature. In other electrolytes, the main problems with 304SS arise because of the current collector electrochemical dissolution. Similarly, the inadequation of aluminum with LiTFSI is not surprising because of a catalyzed oxidation of this metal in such electrolyte [17]. Moreover, we can underline that whatever the substrate nature, no side-reactions were observed when using the aqueous electrolyte 1 M $LiNO_3$.

Table 1
Compatibility between substrate and EC/DMC based electrolytes (the signs ⊗ and ✓ are used when substrate corrosion is observed and not, respectively)

	$LiPF_6$	$LiAsF_6$	$LiBF_4$	LiTFSI	$LiClO_4$
n-Si(0 0 1)/Pt	⊗	✓	⊗	✓	✓
SS304	⊗	⊗	⊗	⊗	✓
Ti	✓	✓	✓	✓	✓
Al	✓	✓	✓	⊗	✓

3.2. Comparison of the electrochemical properties in aqueous and non-aqueous electrolytes

In light of the above results, we performed a cyclic voltamperometry test (scan rate from 0.2 mV s^{-1} to 7.5 mV s^{-1}) using both 1 M $LiNO_3/H_2O$ (the cycling was performed between −0.1 V and 0.8 V vs. SCE) or 1 M $LiClO_4$/EC-DMC electrolytes with a 450 nm thick film. Typical $FePO_4/LiFePO_4$ electrochemical signatures are obtained in both electrolytes [5,8,18] with narrower faradaic peaks for 1 M $LiNO_3/H_2O$, first indication of a faster kinetic (Fig. 3a and b). The measured equilibrium potential is 3.42 V (vs. Li^+/Li) and 0.153 V (vs. SCE) in non-aqueous and aqueous media, respectively. By integrating the peak current, quite similar capacities, (2.06 μAh cm^{-2} vs. 2.27 μAh cm^{-2} in 1 M $LiClO_4$/EC-DMC and 1 M $LiNO_3/H_2O$, respectively) are obtained during the first charge at $v = 0.2$ mV s^{-1} scan rate. The film activity is thus significantly low (by a factor of 10) as compared to the one theoretically expected for this film (26.9 μAh cm^{-2}) [6,7]. Fig. 4a represents the capacity evolution as a function of the scan rate. A capacity decrease is observed by increasing the scan rate owing to the low intrinsic transport properties of $LiFePO_4$ but with a lower fade in 1 M $LiNO_3/H_2O$ (76% of the initial capacity is still recorded at 7.5 mV s^{-1} as compared to 38.2% in 1 M $LiClO_4$/EC-DMC). Independently of the solvent nature, a linear evolution of the current density as a function of the scan rate square root is observed attesting that (i) the redox system is rapid in both electrolytes, and (ii) the de-insertion/insertion kinetic is under diffusion control (Fig. 4b). Interestingly, the slope is three times greater using 1 M $LiNO_3/H_2O$ ($\Delta = 0.135$ mA $s^{0.5}$ cm^{-2} $V^{-0.5}$ vs. 0.042 mA $s^{0.5}$ cm^{-2} $V^{-0.5}$). All of these results indicate a faster electrochemical kinetic using the aqueous electrolyte. Moreover plotting the evolution of the current density vs.

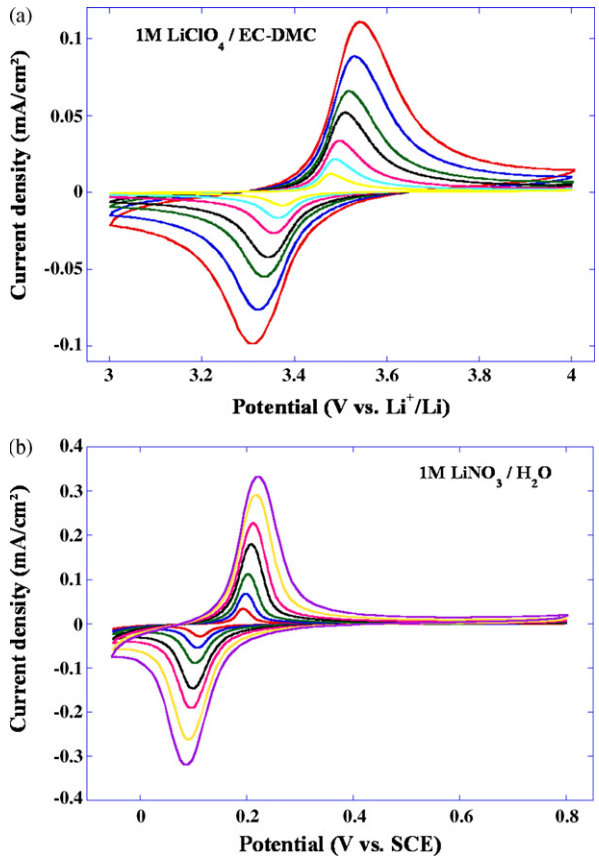

Fig. 3. Cyclic voltamperogram recorded using a 450 nm thick $LiFePO_4$ thin film at different scan rates from 0.2 mV s^{-1} to 7.5 mV s^{-1} in (a) 1 M $LiClO_4$EC/DMC, (b) 1 M $LiNO_3/H_2O$.

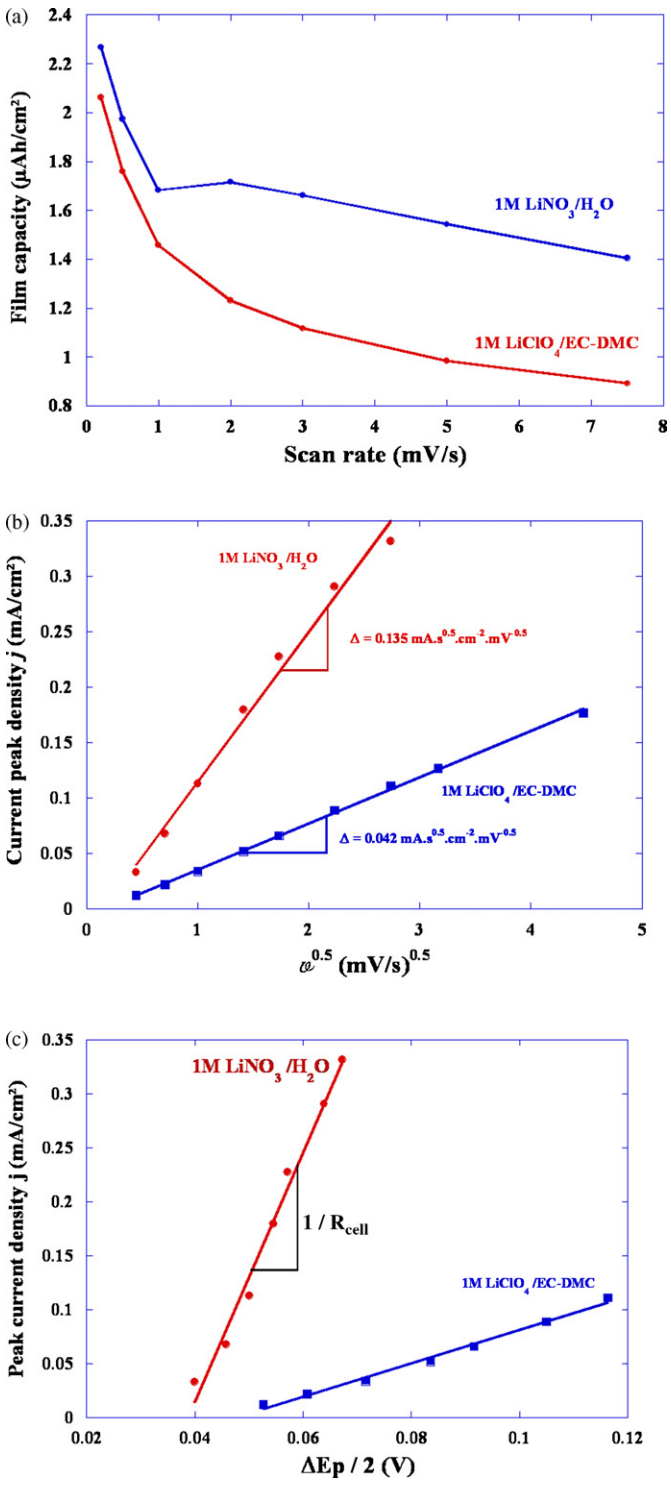

Fig. 4. Electrochemical study of a 450 nm thick $LiFePO_4$ thin film as a function of the scan rate using 1 M $LiNO_3$ H_2O or $LiClO_4$. (a) Evolution of the film capacity during cycling, (b) linear dependency of the current peak density as a function of $v^{0.5}$, (c) linear dependency of the peak current density as a function of ΔEp/2.

ΔEp/2 (with ΔEp the peak separation and ΔEp/2 equivalent to the polarisation of the cell) we also obtain a linear evolution indicating an ohmic behaviour (Fig. 4c). The calculated cell resistances are different by about one order of magnitude (86 Ω cm^2 in 1 M $LiNO_3/H_2O$ as compared to 643 Ω cm^2 in the organic electrolyte). Similar results were reported by Lee and Pyun on $LiMn_2O_4$ thin films [19] confirming the better rate capability recorded in 1 M $LiNO_3/H_2O$. To rule out the major influence of electrolyte conductivity, we have compared the film capacities recorded in galvanostatic mode for the two previous electrolytes together with 0.1 M $LiNO_3/H_2O$ which exhibits a comparable ionic conductivity ($\sigma_{Li^+} = 8.8 \times 10^{-3}$ M) to the perchlorate-based electrolyte (Fig. 5). As expected, using a 0.1 M $LiNO_3/H_2O$ electrolyte induces a decrease (i) in the redox potential of $FePO_4/LiFePO_4$ in agreement with Nernst law [18] and (ii) in the film capacity from 1.77 µAh cm^{-2} to 1.35 µAh cm^{-2} but remaining larger than the one recorded in the organic electrolyte (0.32 µAh cm^{-2}).

In light of these results, the electrochemical kinetic of C-free $LiFePO_4$ thin films seems to be dominated by the charge transfer process. The impedance spectrum ($\Delta E = 20$ mV) recorded in aqueous media displays a semi-arc with a characteristic frequency of 5 kHz and a resistance of ca. 50 Ω cm^2 giving a capacitance of 6.4×10^{-7} F cm^{-2} or 4 mF g^{-1} (assuming the theoretical film density), consistent with a double layer capacitance (Fig. 6). The resistance of this semi-circle can be thus ascribed to the charge transfer resistance. At low frequencies, a Warburg-diffusion behaviour is observed. The impedance response in organic media is remarkably more complex with the convolution of several semi-circles having closed relaxation time

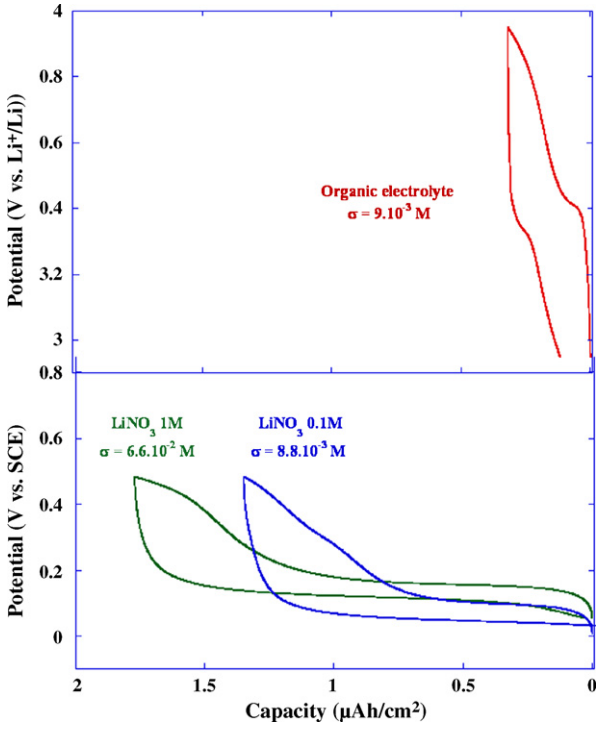

Fig. 5. Comparison of the galvanostatic signatures as a function of the electrolyte for a 450 nm thick $LiFePO_4$ thin film (current density $j = 1\ \mu A\ cm^{-2}$).

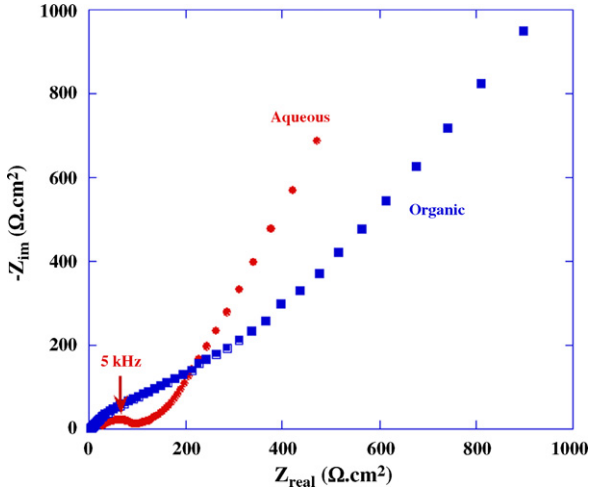

Fig. 6. Electrochemical impedance spectroscopy response recorded using a three-electrode setup for a thin $LiFePO_4$ film 450 nm thick in aqueous and in organic electrolytes.

among which one is most likely linked to a passivation film on the $LiFePO_4$ surface [20]. The formation of polymer/polycarbonate layers similar to the SEI is well established on oxide-based cathode surface and dependent on the surface acid/base properties [21,22]. Moreover, we can notice a clear increase of the global interfacial resistance. In addition to the probable surface layer, this increase could also be linked to (i) the solvation of lithium-ion which is more important in non-aqueous electrolyte as a result of the higher dipole moment of the EC/DMC ($\sim 16 \times 10^{30}$ C m vs. 6.07×10^{30} C m for H_2O) and (ii) a less efficient surface wetability of the EC/DMC. To summarize, the lithium de-insertion/insertion kinetic is mainly controlled by the higher interfacial impedance in 1 M $LiClO_4$/EC/DMC than in $LiNO_3$ 1 M/H_2O. This point clearly emphasizes the benefit of using aqueous electrolyte rather than the actual organic electrolyte for the study of such films.

3.3. Structural and activity vs. Li^+ evolution of in situ made $LiFePO_4$ thin films

We evaluated the influence of electrode thickness (from 70 nm to 270 nm) on the cyclability using $LiClO_4$-based electrolyte in a CV mode ($v = 2\ mV\ s^{-1}$ between 3 V and 4 V). The capacity (normalized by the first cycle capacity) evolution as a function of the film thickness over 150 cycles is reported Fig. 7. It is clear that the film thickness drastically influences the electrode cycling capability. Indeed, the 70 nm thick film capacity decreases by 40% over the first 10 cycles, while the capacity for thicker is doubled over 150 cycles, consistent with the fact that solely a tiny fraction of the film is initially electrochemically active. A similar behaviour was found using 1 M $LiNO_3$/H_2O. Although such films were initially smooth and dense, after 150 cycles, important morphological evolution can be noticed through the appearance of defects on the 150 nm and 270 nm thick films (Fig. 7). The progressive appearance of such surface modifications induces both an increase of triple point numbers (area of electrolyte/electrode/current collector contact) and the contact area between the film and the electrolyte explaining the capacity increase. From a structural point of view, the formation of crevices reveals the existence of noticeable strains released during the $LiFePO_4$/$FePO_4$ phase transition upon cycling, in agreement with recent works on both hexagonal single crystals and on platelet-like particles [23–25]. The release of these strains via electrochemical grinding appears to be beneficial to the electrochemical activity of our films that are in strong interaction with the substrate. Such an observation is not unique as such strains/structural pressure interaction is now well known to have a drastic effect on the electrochemical insertion/de-insertion of lithium as exemplified by the reactivity of rutile TiO_2 [26]. In this latter case, the uptake/removal of Li^+ was triggered by moving from bulk to nano-TiO_2 rutile particles owing to the ability of these latter to easily release the strains/structural tensions upon cycling.

At this point it is legitimate to ask why the above described results apparently contrast with those reported by Iriyama et al. [27] and Song et al. [28] depicting a capacity fading for films thicker than 150 nm. It should be recognized that these films were prepared though a two-step growth route (one step deposition at room temperature + a crystallization step via a post annealing treatment) favouring open morphology, positive attribute to enhance the films electrochemical activity. We further looked at the evolution of the film texture during cycling using HRTEM on a 250 nm thick thin film. To do so, the as-made film was examined prior to cycling (Fig. 8a) and after 150 cycles (Fig. 8b). As we can see, the as-deposited thin film is well crystallized and formed by disoriented nano-sized domains (20–50 nm). After 150 cycles, an important evolution is noticed (Fig. 8b).

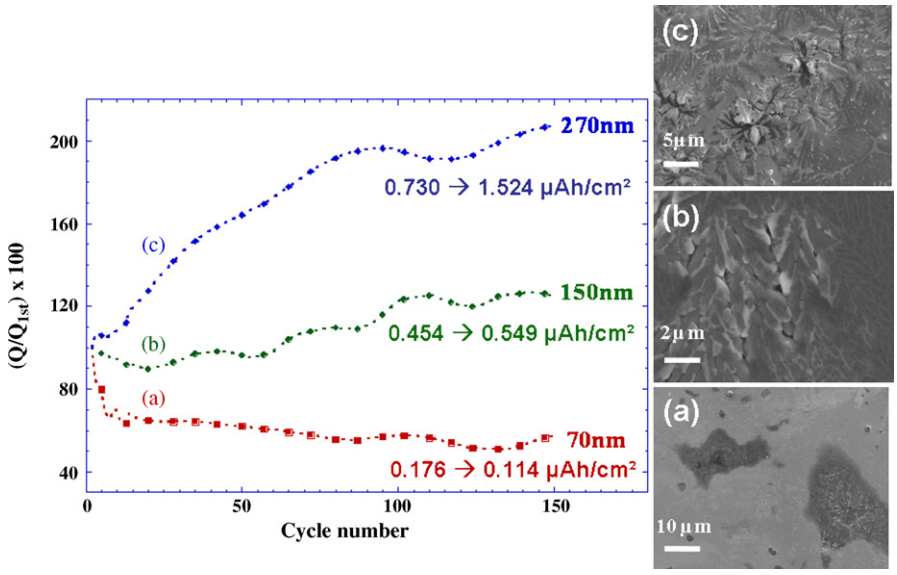

Fig. 7. Capacity evolution (normalized by the 1st cycle capacity) in a cyclic voltamperometry mode ($v = 2\,mV\,s^{-1}$) using 1 M $LiClO_4$ EC/DMC for $LiFePO_4$ thin films of (a) 70 nm, (b) 150 nm, (c) 270 nm thick and SEM images of these films after 150 cycles (the initial and final capacities for each film are reported in inset).

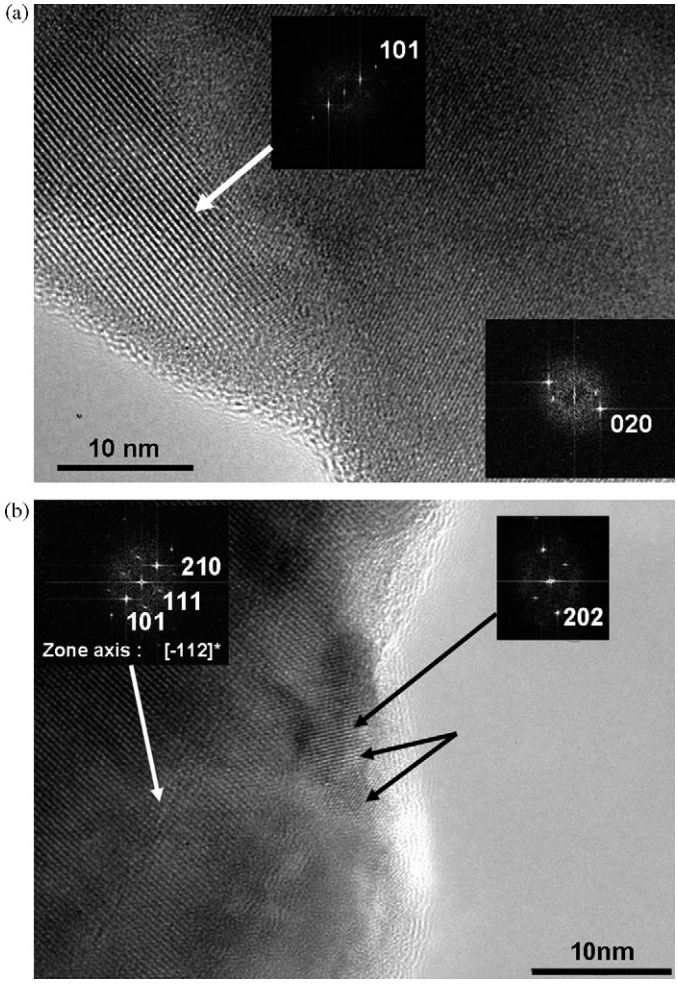

Fig. 8. HRTEM picture of 250 nm thick $LiFePO_4$ thin film (a) initial state (picture adapted from Ref. [7]), (b) after 150 cycles in cyclic voltamperometry mode at $v = 2\,mV\,s^{-1}$ (black arrows illustrate some nanocristallites which were formed).

Indeed, while the core of the films does not change drastically, much smaller crystallized domains together with some defective regions ranging from 4 nm to 10 nm are clearly visible on the sample border edge. This is reminiscent of an electrochemical grinding phenomenon. The region between the core and the ground particle edge most likely defined the depth limit of the film activity (<10 nm) in the used conditions.

4. Conclusion

We first discussed the importance of selecting, in conjunction with the nature of the substrate, the appropriate electrolyte prior to undertaking any electrochemical activity studies of cathode material thin films. Both LiTFSI and $LiClO_4$ EC/DMC electrolytes turn out to be the most friendly when Si(0 0 1)/Pt substrates are used. In contrast, we highlighted a strong corrosion of both *n*-Si(0 0 1)/Pt and 304SS substrates in presence of electrolytes bearing fluorine-based salts. The influence of the solvent nature (aqueous vs. non-aqueous) on the electrochemical properties of $LiFePO_4$ thin films was examined. Significant cell and interfacial resistances decreases were found using aqueous electrolyte (1 M $LiNO_3/H_2O$) enabling a better electrochemical utilization of $LiFePO_4$ thin films. Moreover, we noticed a capacity increase upon cycling for films thicknesses greater than 150 nm, while thinner (70 nm) exhibits 40% capacity loss after 10 cycles. Such a difference was shown to be nested in the onset of defects which develop upon cycling on thick films owing to a less influence of the substrate induced strains upon increasing the film thicknesses. This confirms again the importance of structural strains on the cycling properties, leading to either severe capacity limitations or drastic textural modifications. Although the current work is focussed on $LiFePO_4$ thin films, we believe that most of the observed phenomena are applicable to other poorly conducting inter-

calation materials as long as they can be prepared as thin films.

Acknowledgments

The authors wish to thanks Pr. Hong Li for fruitful discussions.

References

[1] A.K. Padhi, K.S. Nanjundaswamy, J.B. Goodenough, J. Electrochem. Soc. 144 (4) (1997) 1188.
[2] N. Ravet, J.B. Goodenough, S. Besner, M. Simoneau, P. Hovington, M. Armand, Paper 124 Presented at the Electrochemical Society Meeting, Honolulu, HI, October 1999, p. 17.
[3] A. Yamada, S.C. Chung, K. Hinokuma, J. Electrochem. Soc. 148 (3) (2001) A224–A229.
[4] C. Delacourt, P. Poizot, S. Levasseur, C. Masquelier, Electrochem. Solid-State Lett. 9 (7) (2006) A352–A355.
[5] F. Sauvage, E. Baudrin, M. Morcrette, J.-M. Tarascon, Electrochem. Solid-State Lett. 7 (1) (2004) A15.
[6] F. Sauvage, E. Baudrin, L. Gengembre, J.-M. Tarascon, Solid State Ionics 176 (23–24) (2005) 1869.
[7] F. Sauvage, L. Laffont, J.-M. Tarascon, E. Baudrin, Solid State Ionics 178 (1–2) (2007) 145.
[8] M. Manickam, P. Singh, S. Thurgate, K. Prince, J. Power Sources 158 (2006) 646.
[9] C.H. Mi, X.G. Zhang, H.L. Li, J. Electroanal. Chem. 602 (2) (2007) 245.
[10] W. Li, J.R. Dahn, D.S. Wainwright, Science 264 (1994) 1115.
[11] J.-M. Tarascon, D. Guyomard, Solid State Ionics 69 (3–4) (1994) 293–305.
[12] M. Moshkovich, M. Cojocaru, H.E. Gottlieb, D. Aurbach, J. Electroanal. Chem. 497 (2001) 84–96.
[13] D. Aurbach, Y. Gofer, J. Electrochem. Soc. 138 (1991) 3529.
[14] D. Aurbach, A. Zaban, A. Schechter, Y. Ein-Eli, E. Sinigrad, B. Markovsky, J. Electrochem. Soc. 142 (9) (1995) 2873–2881.
[15] V. Lehmann, R. Stengl, A. Luigart, Mater. Sci. Eng. B 69–70 (2000) 11–22.
[16] H.C. Shin, J.A. Corno, J.L. Gole, M. Liu, J. Power Sources 139 (1–2) (2005) 314–320.
[17] L.J. Krause, W. Lamanna, J. Summerfield, M. Engle, G. Korba, R. Loch, R. Atanososki, J. Power Sources 68 (1997) 320–325.
[18] F. Sauvage, J.-M. Tarascon, E. Baudrin, Anal. Chim. Acta, submitted for publication.
[19] J.-W. Lee, S.-I. Pyun, Electrochim. Acta 49 (2004) 753–761.
[20] M. Koltypin, D. Aurbach, L. Nazar, B. Ellis, Electrochem. Solid State Lett. 10 (2) (2007) A40–A44.
[21] D. Aurbach, K. Gamolsky, B. Markovsky, G. Salitra, Y. Gofer, U. Heider, R. Oesten, M. Schmidt, J. Electrochem. Soc. 147 (2000) 1322.
[22] K. Edström, T. Gustafsson, J.O. Thomas, Electrochim. Acta 50 (2004) 397–403.
[23] G. Chen, X. Song, T.J. Richardson, Electrochem. Solid State Lett. 9 (6) (2006) A295–A298.
[24] D. Wang, X. Wu, Z. Wang, L. Chen, J. Power Sources 140 (2005) 125–128.
[25] N. Meethong, H.Y. Shadow Huang, S.A. Speakman, W.C. Carter, Y.M. Chiang, Adv. Funct. Mater. 17 (2007) 1115–1123.
[26] E. Baudrin, S. Cassaignon, M. Koelsch, J.-P. Jolivet, L. Dupont, J.-M. Tarascon, Electrochem. Commun. 9 (2007) 337.
[27] Y. Iriyama, M. Yokoyama, C. Yada, S.K. Jeong, I. Yamada, T. Abe, M. Inaba, Z. Ogumi, Electrochem. Solid State Lett. 7 (10) (2004) A340–A342.
[28] S.W. Song, R.P. Reade, R. Kosteki, K.A. Striebel, J. Electrochem. Soc. 153 (1) (2006) A12–A19.